HHS Public Access

Author manuscript

Glia. Author manuscript; available in PMC 2015 April 30.

Published in final edited form as:

Glia. 2009 April 1; 57(5): 510–523. doi:10.1002/glia.20780.

Quantitative analysis of mitotic Olig2 cells in adult human brain and gliomas: implications for glioma histogenesis and biology

Wootack Rhee[1,*], **Sutapa Ray**[1], **Hideaki Yokoo**[2], **Megan E. Hoane**[1], **Chong C. Lee**[1], **Andrei M. Mikheev**[1], **Philip J. Horner**[1], and **Robert C. Rostomily**[1,^]

[1]Department of Neurological Surgery, University of Washington School of Medicine, Seattle WA

[2]Department of Pathology, Gunma University Graduate School of Medicine, Maebashi, Japan

Abstract

The capacity of adult human glial progenitor cells (AGPs) to proliferate and undergo multipotent differentiation positions them as ideal candidate cells of origin for human gliomas. To investigate this potential role we identified AGPs as mitotically active Olig2 cells in non-neoplastic adult human brain and gliomas. We conservatively estimated that 1 in 5,000 human temporal lobe neocortical gray or sub-cortical white matter cells is mitotic. Extrapolating from a mean Olig2/Mib-1 labeling index (LI) of 52% and total cell number of 100 billion, we estimated the overall prevalence of mitotic Olig2 AGPs in non-neoplastic human brain parenchyma at 10 million. These data identify a large reservoir of Olig2 AGPs which could be potential targets for human gliomagenesis. The vast majority of mitotic cells in Grade II and III gliomas of all histologic sub-types expressed Olig2 (mean LI 75%) but rarely S100B (LI 0.6%), identifying the Olig2 cell as a distinct contributor to the proliferating cell population of human gliomas of both oligodendroglial and astrocytic lineages. In the most malignant grade IV glioma, or glioblastoma multiforme (GBM), the prevalence of Olig2/Mib-1 cells was significantly decreased (24.5%). The significantly lower Olig2/Mib-1 LI in GBMs suggests that a decrease in the prevalence of Olig2 cells to the total mitotic cell pool accompanies increasing malignancy. The novel framework provided by this quantitative and comparative analysis supports future studies to examine the histogenetic role of Olig2 AGPs in adult gliomas, their potential contribution to the tumor stroma and the molecular role of Olig2 in glioma pathogenesis.

Keywords

glial progenitor; gliomagenesis; transcription factor; bHLH; Olig2

INTRODUCTION

The recent detection of glial tumor stem cells has driven interest in the role of immature neural cells as targets for gliomagenesis. The precise identity of glioma cell(s) of origin

^to whom correspondence should be addressed, Robert C. Rostomily, MD, Department of Neurological Surgery, University of Washington, Room RR744, Box 356470, 1959 NE Pacific Street, Seattle, WA, USA 98195-6470, Phone 206-543-3570, fax 206-543-8315, rosto@u.washington.edu.

*current address- University of Ulsan College of Medicine, Department of Neurosurgery, Gangneung Asan Hospital, Korea

remains unclear and although much attention has been focused on adult neural stem cells (NSCs), the recent characterization of adult glial progenitors (AGPs) in the human brain expands the range of possible immature neural cell types that could generate human gliomas. Human gliomas express markers associated with both cell types and animal models that target either NSCs or AGPs faithfully recapitulate the neuropathologic features of human gliomas.

NSCs and AGPs both exhibit properties reminiscent of human gliomas including multipotent differentiation, migration and proliferation, but differ in many fundamental ways. Unlike NSCs that self-renew and generate both neurons and glia *in vivo*, AGPs have limited replicative potential and preferentially produce oligodendroglia *in vivo* (Nunes et al 2003; Arsenijevic et al. 2001; Goldman 2003). Also, AGPs are diffusely distributed throughout the neocortex and sub-cortical white matter (SCWM), while NSCs are localized within distinct germinative zones of the SVZ and sub-granular zone of the hippocampus (Nunes et al 2003; Arsenijevic et al. 2001; Goldman, 2003). Although adult NSCs and AGPs likely represent a diverse spectrum of lineally related cells with partially overlapping localization and physiologic functions, their distinct phenotypes suggest that they may contribute uniquely to the generation of human gliomas.

The presence of AGPs in normal rodent and human brain that exhibit an immature phenotype defined by distinct protein and transcription factor profiles also supports their potential roles in glioma biology (Goldman 2003; Horner et al. 2002; Liu and Rao 2004). In adult rodent neocortical gray matter and SCWM, the majority of mitotic cells demonstrate a glial progenitor phenotype (Dawson et al. 2003; Gensert and Goldman 2001). Multipotent glial progenitors with proliferative capacity *in vitro* have been isolated from adult human SCWM (Nunes et al. 2003; Scolding et al. 1999; Scolding et al. 1995) and neocortex (Arsenijevic et al. 2001). Two factors commonly expressed by AGPs, NG2 and Olig2, define the most proliferative population of cells outside neurogenic regions of the rodent brain (Dawson et al. 2003; Marshall et al. 2005). As in rodents, cells expressing the NG2 proteoglycan in humans are distributed diffusely throughout the gray and SCWM (Chang et al. 2000; Shoshan 1999). The co-expression of Olig2 in most NG2 cells in the rodent CNS also supports the notion that Olig2 defines a population of glial progenitor cells (Ligon et al. 2006b). Of importance cells with AGP phenotypes have been linked to gliomagenesis both experimentally and in human tissue samples.

Barnett et al (Barnett et al, 1998) directly transformed NG2 expressing rat AGPs (O2A cells) in vitro that upon implantation into syngeneic host brains produced malignant glial tumors with features similar to human glioblastoma. PDGF over-expressing retrovirus injected into rodent white matter preferentially infects NG2 AGPs to generate malignant gliomas similar to human GBM that express Olig2 in the vast majority of transduced tumor cells (Assanah et al, 2006). Of importance, Olig2 and NG2 proteins are both expressed in human gliomas (Shoshan et al. 1999; Ligon et al. 2004) and the expression of Olig2 in gliomas of either astrocytic or oligodendroglial differentiation is consistent with the inherent capacity of AGPs for multipotent glial differentiation (Ligon et al. 2004; Mokhtari et al. 2005).

The phenotype and existence of mitotic AGPS in human brain and the observations above in animal and human gliomas supports the importance of AGPs to human glioma formation and biologic phenotype. Despite this, no study has attempted to rigorously analyze the prevalence of AGPs, particularly in the mitotic pool of neural cells outside the CNS germinative zones, or correlated such data with similar analysis in human glioma tissue samples. In this study we established the prevalence of mitotic cortical Olig2 AGPs in non-neoplastic human brain and, by comparative analysis of mitotic Olig2 cells in human gliomas, investigated their possible role(s) in glioma biology. The comparative prevalence of mitotic AGPs in non-neoplastic brain and human gliomas supported a potential histogenetic role for AGPs in human gliomas and suggested additional functional contributions to malignant glioma phenotype.

MATERIALS AND METHODS

Tissue samples and patient characteristics

Temporal lobe non-neoplastic brain and glioma tumor tissues were obtained in compliance with an approved University of Washington Human Subjects protocol from patients undergoing surgical resection for epilepsy, exposure to benign brain tumors or primary gliomas. Macroscopically evident regions of cortical gray matter (GM) and sub-cortical white matter (WM) from each patient were immediately dissected, fixed in formalin and mounted in random orientation in paraffin blocks to eliminate structural bias in cell densities. Two separate sets of paired samples were generated (Table 1); the first set of paired GM/WM samples from 14 patients (Panel 1) was processed for analysis of Mib-1 labeling indices (data summarized in Table 2), and the second set of paired GM/WM samples from 12 patients (Panel 2) was used to quantify Olig2 expression in Mib-1 expressing cells (data summarized in Table 3). Glioma samples were retrieved from archived formalin-fixed and paraffin-embedded samples. H&E histological verification was performed for all non-neoplastic and glioma samples.

Immunohistochemistry

IHC analysis on non-neoplastic brain sections included Mib-1, Olig2/Mib-1, Olig2/NG2 and for gliomas Olig2/Mib-1 and S100B/Mib-1. All IHC was performed on 6μm formalin-fixed and paraffin- embedded sections except those used for Olig2/NG2 IHC. After deparaffinization and rehydration all sections were subjected to antigen retrieval by microwave heating for 4 min at 100% power, then 10 min at 10% power in 10mM Citrate buffer pH 6.0 and treated to reduce auto-fluorescence by immersion in 1% Sudan-Black B solution for 5 minutes, brief immersion in 80% ETOH and PBS rinse (Schnell et al. 1999). Sections were then blocked with 2% horse serum and 0.3% triton-X, incubated in primary antibody over night at 4°C and 1hr in secondary antibody at room temperature followed by DAPI (1:1000) counterstaining. Sections were mounted (Fluoromount G, Southern Biotec, Birmingham, AL, USA) and light protected until analyzed. For Olig2/NG2 IHC, 40 μm sections from 2 separate samples of fresh frozen brain including both gray and white matter were fixed in 4% paraformaldehyde. After blocking with 10% horse serum slides were incubated for 48 hours at 4°C with the NG2 primary antibody. The primary antibodies and corresponding secondary antibodies used are as follows: Mib-1 antibody (DAKO 1:500)

visualized by application of FITC donkey anti-mouse secondary antibody (Jackson ImmunoResearch, West Grove, PA, USA; 1:500). Olig2 polyclonal rabbit antibody (1:3000) was kindly provided by H. Yokoo (Yokoo et al. 2004), and visualized with biotinylated goat anti-rabbit secondary antibody (Vector Lab, Burlingame, CA, USA; 1:500) and rhodamine Red-X Conjugated streptavidin (Molecular Probes, Eugene, OR, 1:1000). NG2 primary antibody (BD Biosciences, San Jose, CA, 1:400 dilution) visualized with anti-mouse biotinylated secondary antibody (Vector Lab; 1:500) and streptavidin (Molecular Probes; 1:1000); avidin-biotin block was used per manufacturer's protocol (Sigma, St. Louis, MO), before double labeling with Olig2. S100B rabbit polyclonal antibody (Swant, Bellinzona, Switzerland, 1:500) visualized as Olig2 above. Guinea pig GFAP polyclonal antibody (Advanced ImmunoChemical Inc., 1:500) visualized with donkey anti-GP Cy5 secondary (Jackson, 1:400). Mouse monoclonal CNPase antibody (Sigma, 1:200) visualized as Mib1 above. Mouse monoclonal Nkx2.2 antibody (Developmental Studies Hybridoma Bank, University of Iowa, Iowa City, IA, USA,1:200) labeled with Horse anti-mouse biotin (Vector, 1:250) followed by NeutrAvidin 488 conjugate (Molecular Probes, 1:500).

Confocal microscopy

Prior to cell counting with fluorescent microscopy, the co-localization and patterns of immunoreactivity for Olig2/Mib-1 and Ng2/Olig2 in non-neoplastic brain and Olig2/Mib-1 in selected glioma samples were analyzed by confocal microscopy to confirm appropriate cellular localization and specificity of double-labeled cells. Confocal images were collected on a BioRad radiance microscope (Hercules, CA). Images were imported into Volocity (Improvision, Lexington, MA) to generate compressed z-stacks and 3-dimensional and orthogonal views. Photoshop (Adobe Systems, San Jose, CA) was used to crop and create figure montages from the imported images.

Cell counting in non-neoplastic brain

Mib-1 LI- In a set of 14 paired gray and SCWM samples (Panel 1, Table 1) Mib-1 immunoreactive cells were detected by fluorescent microscopy with a motorized Zeiss Axiovert 200M inverted microscope at 20× magnification. The entire section was analyzed by manually moving the "Z" stage. Digital images were captured of all microscopic fields with Mib-1 cells (Roper HQ camera, Roper Scientific, Duluth, GA, USA) and stored using Slide Book image analysis software (version 4.01.40; Intelligent Imaging Innovations, Inc., Atlanta, GA). The total number of Mib-1 cells was recorded using Image J public domain image analysis software (http://rsb.info.nih.gov/ij). Cells were considered positive if staining was distributed within the confines of a DAPI-delineated nucleus. Most positive cells demonstrated intense homogeneous fluorescence, but due to intranuclear redistribution of Ki-67 protein during different phases of the cell cycle (Verheijen et al. 1989), some positive cells had variable intensity or punctate staining patterns. Mib-1 staining unequivocally co-localized to DAPI nuclei within distinct vascular structures (characterized by either a circular, longitudinal or branching pattern of elongated endothelial nuclei) were excluded from the analysis. A representative Mib-1 stained nucleus from a non-neoplastic brain is shown in Figure 1. *Total cell counts*- The total cell count for each section was estimated to allow determination of the Mib-1 LI (#Mib-1 cells/total cell number). The number of 20× microscopic fields comprising a section was determined using Slidebook (III; Atlanta, GA)

image analysis software and the whole area of the specimen was measured using a Duoscan T2500 slide scanner (AGFA, Germany). Except for small samples, at least ten fields comprising 8.4–29% of the total section area were counted. Sections containing Mib-1 cells were counted while the remaining fields for each section were determined by random number generation using Slidebook (III, Atlanta, GA). To verify that inclusion of fields containing Mib-1 cells did not introduce bias into the estimations of total cell counts, a second observer estimated total cell counts using only randomly selected fields (see statistical analysis below). Each DAPI-stained nucleus was marked using Image J (NIH shareware) to prevent recounting and randomly oriented samples were used to reduce bias created by regional differences in cell density, particularly in gray matter. *Olig2/Mib-1 LI*- To allow analysis of Olig2 expression in a larger number of non-neoplastic gray and SCWM mitotic cells, a second set of samples was used ("Panel 2", table 3) that had larger areas than those used for the Mib-1 LI analysis. For each sample, 2–4 adjacent sections were counted at 40× magnification. Co-expression of Olig2 was determined for each Mib-1 immunoreactive cell. The LI was calculated as follows (# Mib-1/Olig2 cells/ total # Mib-1 cells × 100). A cell was considered positive for Olig2 expression only when the fluorescent signal was stronger than the background of non-oligodendroglial cells and its morphological characteristics were consistent with a nucleus that could be confirmed by DAPI fluorescence signal. *Olig2/Ng2*- We analyzed co-expression of Olig2 and NG2 cell in 2 separate samples of fresh frozen brain including both gray and white matter. Cells were considered NG2 positive when immunoflourescent signal surrounded or was in continuity with a DAPI-stained nucleus. These cells were then checked for the presence of Olig2 nuclear immunoreactivity. Co-localization of signal was analyzed at 40× magnification and confirmed by confocal microscopy. Five hundred randomly selected cells were counted and the percentage of NG2 cells co-expressing Olig2 was recorded.

Cell counting in human gliomas

Microscopic fields were analyzed at 40× magnification in a non-overlapping random checkerboard configuration (approximately one-half of the total sample area) to identify Mib-1 immunoreactive cells. For each Mib-1 cell, the presence or absence of Olig2 or S100 beta immunoreactivity was recorded. *Olig2/Mib-1*- The same Olig2/Mib-1 double-label immuno-staining technique and criteria for identifying positive cells as described for non-neoplastic brain was applied to the human glioma samples. *S100B/Mib-1*- The localization of S100B in either the nucleus or cytoplasm has been documented in prior studies (Deloulme et al. 2004; Hachem et al. 2005; Hayashi et al. 1991). Cells were considered to be double-labeled for Mib-1 and S100B when either nuclear and/or cytoplasmic staining intensity for S100B was above tissue background and unambiguously localized to a Mib-1 positive nucleus.

Statistical analysis

Two-tailed paired t-tests were used to compare measurements of Mib1 LI, cell density and Olig2 Mib1 LI taken from both gray and white matter samples from non-neoplastic human brains. Additional effects due to patient characteristics such as age, gender, pathology and prior grid placement were individually tested using a repeated measures ANOVA model that employed a random effect due to subject. (Modelling was done with the 'proc mixed'

procedure available in SAS). Measurements of Mib1 LI and Olig2/MIb1 LI taken from tumors were analyzed using a one-way ANOVA with a Tukey post-hoc multiple comparison test for significance between groups. Differences were considered significant if the p value was less than 0.05. *Inter-observer error*- To determine the variability between observers in data collection, a second observer blindly counted randomly selected samples using established criteria and techniques (6 GM and 4 WM for cell density; 6 sections each of GM and WM for Mib-1 LI; 6 GM and 4 WM for Olig2/Mib-1 LI in non-neoplastic brain; and Olig2/Mib-1 LI and S100B/Mib-1 LI from 2 astrocytomas, 3 oligodendrogliomas, 1 mixed oligoastrocytoma and 3 GBM). No significant differences in the means or variance were found for cell density values for GM or WM samples using unpaired t-tests and an F-test to compare variances between observers. All other comparisons were performed using a paired t-test and evaluation of correlation. In all analyses, the correlations between the comparative data sets were highly significant while significant differences in mean values were not identified. The correlations and their p-values for each data set were as follows: Mib-1 cell numbers in non-neoplastic brain, ($r= 0.8913$, $p<0.0001$), Olig2/Mib-1 double-labeled cell counts from non-neoplastic brain ($r=0.9441$, $p<0.0001$), Olig2/Mib-1 LI in gliomas ($r=0.9885$, $p<0.0001$) and S100B/Mib-1 LI for gliomas ($r= 0.9952$, $p<0.0001$).

RESULTS

Proliferating cells in non-neoplastic human brain

In the set of non-neoplastic human brain samples used to quantify Mib-1 LI (Panel 1, table 1), no associations were noted between other variables that might affect Mib-1 LI such as patient age, gender, underlying pathology and prior grid placement even after adjusting for the GM/WM variable (data not shown). The overall mean Mib-1 LI for all non-neoplastic brain samples was 0.04%, or one mitotic cell in 2500. The mean Mib-1 LI was higher in samples with prior grid placement (mean LI 0.074%) versus no prior grid (mean 0.021%) but this difference did not reach statistical significance (table 2). Of the total number of Mib-1 cells counted in all 28 samples, 59% were concentrated in two samples from a patient with prior grid placement. The marked increase in the Mib-1 LIs in these samples compared with all other samples (5-fold higher than next highest GM Mib-1 LI and 3-fold higher than next highest WM Mib-1 LI) suggested that a severe reaction to grid placement occurred in this patient. Since this is less likely to reflect the normal physiologic state of mitotic activity in the brain, we recalculated the Mib-1 LI to exclude these “outliers” and arrived at a mean Mib-1 LI of 0.022% for individual GM and WM Mib-1 LIs (approximately one Mib-1 cell per 4500 total cells) or 0.026% (approximately one Mib-1 cell per 3800 total cells) when the Mib-1 LI is calculated from cell counts pooled from all samples. These values are very similar to the mean of individual Mib-1 LIs (0.21%) from non-grid samples and presumably more closely represents normal physiologic mitotic activity.

The degree of regional variability within individual samples was addressed by counting Mib-1 cells from equally sized serial sections taken at 100μM intervals from 3 large epilepsy brain samples containing both GM and WM. The Mib-1 cell counts for each sample ranged from 2 to 14 (2, 13, 7, 14, 10), 1 to 6 (6, 2, 4, 1, 2, 6), and 3 to 11 (8, 9, 11, 9, 3, 4).

Excluding the two outlying samples discussed above, this regional variability of mitotic activity (3.7-7 fold) is similar to that observed among samples in panel 1 (Table 1).

In the course of determining Mib-1 LIs we also quantified total cell counts and cell densities (Table 2). Mean cell densities were significantly higher in WM (1550 cells/mm2) than GM (1114 cells /mm2) and comparable to previous reports (Nedergaard et al. 1984). Variability in cell density was greater in samples of white matter (S.D. +/−504) than gray matter (S.D. +/− 203) which may be due to the effects of chronic epilepsy or tissue fixation (Kretschmann et al. 1986; Mouritzen Dam 1979). Because the fresh sample volumes were not recorded, we could not correct for tissue contraction due to fixation, but this may account for variability in white matter cell densities. Together these results provided new insight to indicate the level of and variability of mitotic activity in non-neoplastic human brain in GM and WM outside of the germinal zones.

Olig2 expression in non-neoplastic proliferating cells

To identify proliferating cells with an AGP immunophenotype in the non-neoplastic adult brain we performed double-label IHC for Mib-1 and the glial progenitor marker Olig2 in a second panel (Panel 2, Table 1) of non-neoplastic brain samples (summarized in Table 3 and Figure 4). Olig2 expression in mitotic cells outside the germinal zones provided unambiguous identification of a glial progenitor cell as opposed to terminally differentiated oligodendrocyte, and its nuclear staining pattern facilitated detection of Olig2/Mib-1 double-labeled cells (Figure 3). Overall, Olig2 cells represented the majority of Mib-1-expressing cells in non-neoplastic brain samples (mean Olig2/Mib-1 LI 52.2%; the prevalence of Olig2/Mib-1 cells was significantly higher in white matter (mean Olig2/Mib-1 LI of 66.4%) than gray matter (mean Olig2/Mib-1 LI of 38.0%). No major differences were noted for Olig2/Mib-1 LI between grid and non-grid samples (data not shown). Overall our results indicated that a mitotic AGP, defined by Olig2 expression, comprises slightly over half of all proliferating cells in non-neoplastic human temporal lobe differentially distributed with greater prevalence in SCWM than neocortex.

Olig2/Mib-1 and S100B/Mib-1 co-expression in human gliomas

We hypothesized that the proliferating Olig2 AGP is a target cell for gliomagenesis and therefore analyzed expression of Olig2 in mitotic cells from a panel of human glial neoplasms. The prevalence of Olig2 proliferating cells was compared with that of S100B proliferating cells to provide a comparison of mitotic activity in cells of astroglial lineage. While S100B expression is reported in some neurons and oligodendrocyte progenitors (Vives et al. 2003; Deloume et al. 2004; Hachem et al. 2005) we found a high correlation between S100B and the astroglial specific marker GFAP expression (Supplemental data Figure 1). We chose not to use GFAP for the cell counts because its cellular localization in cell processes makes it more difficult to associate its expression to a specific cell than S100B. In all, we analyzed 11 WHO grade II gliomas (4 astrocytoma, 5 oligodendrogliomas and 2 mixed oligoastrocytoma), 11 WHO grade III gliomas (4 astrocytoma, 3 oligodendrogliomas and 4 mixed oligoastrocytoma) and 9 grade IV glioblastomas.

Our results indicated that the Olig2/Mib-1 glial progenitor immunophenotype comprises the vast majority of proliferating cells in grade II and III gliomas but a significantly smaller proportion of mitotic cells in grade IV neoplasms. In grade II and grade III gliomas, Olig2 was commonly co-expressed in proliferating cells. The mean Olig2/Mib-1 LI for all grade II gliomas was 67.7 % (range 21%-90%) with means of 79.5%, 56.4% and 72.5% for astrocytoma, oligodendroglioma and mixed glioma, respectively. The mean Olig2/Mib-1 LI for all grade III gliomas was 83.6 % (range 65%-95%) with means of 88.8%, 79.3% and 81.8% for astrocytoma, oligodendroglioma and mixed glioma, respectively. For grade IV glioblastoma, the individual Olig2/Mib-1 LIs demonstrated greater variability (range 6–63%) and significantly lower mean Olig2/Mib-1 LIs (24.9%; p=0.001) than grade II and III gliomas. By contrast, S100B/Mib-1 cells were only encountered in 2 grade II, 6 grade III and 2 grade IV samples with the highest LI being 6%. Representative images of Olig2/Mib-1 and S100B/Mib-1 cells from glioma samples are shown in Figures 5 and 6 and Supplemental data Figure 2, and data for Olig2/Mib-1 and S100B/Mib-1 is summarized in Table 3 and Figure 7.

AGP immunophenotype

To better establish the relationship between Olig2/Mib-1 cells detected in non-neoplastic brain and gliomas we investigated their co-expression with astroglial markers GFAP and S100B, and other markers expressed by AGPs, NG2, CNPase and NKX2.2 (Colin et al. 2007; Rousseau et al. 2006). Figure 8 summarizes the general immunophenotype of the AGP population we have identified in non-neoplastic human brain and human gliomas of various types and grades. Adjacent sections from the same tissue sample block were stained with H&E to confirm pathology and then stained for Olig2/Mib1, S100/Mib1 and GFAP/Mib1 by IHC. Our data suggests that AGPs are a mitotic cell population that expresses Olig2 but rarely S100 or GFAP.

To determine the potential overlap between the Olig2 AGP and the neocortical and SCWM NG2 AGP described in rodents and humans, we examined co-expression of Olig2 in 500 NG2 cells from 2 large sections of human temporal lobe containing both neocortex and SCWM obtained from epilepsy patients (Figure 9). The pooled results showed that approximately 62% of NG2 cells co-expressed Olig2 (data not shown). Given that Olig2 and NG2 are also expressed in non-overlapping cell types (NG2 in pericytes and microglia and Olig2 in post-mitotic oligodendroglia), this finding and the high prevalence of Olig2 proliferating cells in the adult non-neoplastic brain, together suggest that a large pool of human AGPs in neocortex and SCWM may be defined by co-expression of Olig2 and NG2. In our glial tumor samples, NG2 Olig2 colocalization was also observed, although not quantified (Supplemental data Figure 3).

We also looked at co-expression of other markers expressed by glial progenitors, Nkx2.2 and CNPase with Olig2 and further compared and contrasted co-expression of astroglial markers S100B and GFAP by IHC. We found little to no expression of GFAP in Olig2 cells and little to no expression of S100B in mitotic cells, whereas both these astroglial markers seemed to colocalize considerably with each other (See supplemental data Figure 1). Together these findings indirectly imply that S100B/Olig2 expression would be expected at

low levels. Because our Olig2 and S100B antibodies are raised in the same host species, direct double-labeling was not possible. We found a large overlap in Olig2 and Nkx2.2 expression in the non-neoplastic brain and a sub-population of the Olig2 positive cells were found to express CNPase (Supplemental data Figure 3). Most importantly, all these observations of AGP immunophenotype in the non-neoplastic brain also held true for human gliomas (Supplemental data Figure 3). These data demonstrate a similar immunophenotype for Olig2/Mib-1 cells in non-neoplastic brains and glial tumors.

DISCUSSION

The data presented here provides the only comprehensive comparison between the prevalence of mitotic AGP cells in non-neoplastic human brain samples and human glioma tissues and provides insight into the role of the Olig2 AGP in the histogenesis of human gliomas as well as potential additional functional role(s) in glioma biology. The relative abundance of proliferating Olig2 AGPs in non-neoplastic human brain demonstrates that a large pool of these potential glioma target cells exists in the adult brain. Furthermore, the predominance of this same Olig2 immunophenotype in mitotic glioma cells of grade II and III (regardless of histologic type) and a smaller proportion of grade IV gliomas, supports important roles for the Olig2 AGP in the histogenesis and pathogenesis of human gliomas.

Cell proliferation in non-neoplastic human temporal lobe

We previously reported S+G2/M-phase fractions of 1.7% from freshly processed (Mesiwala et al. 2004) and 2.3% from formalin-fixed paraffin-embedded samples of epileptic brain (Rostomily et al. 1997) using flow cytometric techniques. However, comprehensive quantification of mitotic activity *in situ* in human non-neoplastic brain tissues using immunohistochemical techniques is lacking. The existing data, consisting of small numbers of non-neoplastic brain controls used for glioma studies, report absent (Park and Suh 2003; Kato et al. 2003) or low (0 +/− 0.01%) (Weil et al. 2001) mitotic acitivity. Here, for the first time, we rigorously characterized basal mitotic activity within human non-neoplastic brain samples and found that a sizeable pool of mitotic cells resides in human adult temporal lobe.

Given our findings of one mitotic cell among every 2500 to 5,000 cells in adult human non-neoplastic gray matter and SCWM cells and an estimated 100 billion cells total in human gray and SCWM (Miller et al 1980; Pakkenberg and Gundersen 1997; Pelvig et al; 2003) a conservative estimate places the prevalence of mitotic cells within these brain regions at 20 million. Since these estimates are based largely on epileptic tissue samples, their direct application to the setting of truly normal brain must be interpreted with caution. For instance, the impact of chronic seizures on cell proliferation is not known. Nevertheless, given the obvious limitations that restrict ready acquisition of “truly normal” brain, the present data set does provide significant insight into the resting mitotic activity of the non-neoplastic human brain. Of importance, this estimate indicates that a sizeable pool of mitotic cells and potential glioma target cells exists within the brain parenchyma outside of deep structures and germinal zones of the SVZ and hippocampus.

Prevalence of Olig2 glial progenitors in adult non-neoplastic brain

Just over 50% (40% in gray matter and 70% in SCWM) of the mitotic cells in non-neoplastic human temporal lobe expressed Olig2. Extrapolating as above, the estimated prevalence of mitotic Olig2 AGPs is 10 million and supports their numerical relevance as a candidate glioma target cell. Although Olig2 has diverse functions in early development to specify multiple cell types (spinal cord motor neurons and oligodendroytes, e.g.), in adult rodent neocortical gray matter and SCWM, Olig2 is expressed in AGPs (Marshall et al. 2005; Menn et al. 2006) and post-mitotic oligodendrocytes (Ligon et al. 2004). These adult Olig2 AGPs are important for the generation of NG2 AGPs (Ligon et al, 2006) and mature oligodendrocytes (Ligon et al 2006; Marshall et al 2005). Our interpretation of mitotic Olig2 cells as AGPs is supported by the findings of Olig2 co-expression in 62% of NG2 cells and Olig2 co-expression with additional markers expressed by AGPs, NKX2.2 and CNPase, but not with the astroglial marker GFAP. NG2 is expressed in cells widely dispersed in human brain (Shoshan et al. 1999) with characteristics of multipotent AGPs (Nunes et al. 2003; Goldman 2003). In rodent cerebral cortex and SCWM of the corpus callosum NG2 cells comprise approximately 74% of mitotic cells (Dawson et al. 2003). In light of these experimental studies our data supports the identity of mitotic Olig2 cells as AGPs that overlap with previously identified NG2 AGPs and together form a sizeable pool of potential glioma target cells.

Immunophenotype of mitotic human glioma cells

Despite the central importance of cell proliferation in glial oncogenesis, the identity of proliferating cells in human gliomas has not been well characterized. Mitotic GFAP (Kros et al. 1996) and Olig2-expressing (Mokhtari et al. 2005; Yokoo et al. 2004) cells have been observed in oligodendrogliomas but not quantified and Ligon et al, quantified proliferating Olig2 cells in grade IV GBMs alone (Ligon et al. 2007). Here, we quantified the prevalence of mitotic Olig2 cells in a comprehensive panel of human gliomas and found that the vast majority of mitotic cells co-expressed Olig2 in grade II and grade III gliomas, regardless of histologic type, and that the Olig2/Mib-1 LI was significantly reduced in grade IV glioblastomas.

Unlike Olig2, S100B was virtually absent from proliferating cells in human gliomas of any grade or histologic type. S100B is commonly co-expressed with GFAP and has been traditionally used to identify astrocytes (Boyes et al. 1986) although it has recently been detected in neurons and NG2+ oligodendroglial precursor cells (Deloulme et al. 2004; Hachem et al. 2005; Vives et al. 2003). S100B is expressed in tumor cells of grade II and III astrocytomas and in oligodendrogliomas (Hayashi et al. 1991; Van Eldik et al. 1986), with reduced expression in GBM (Camby et al. 1999; Hayashi et al. 1991). Although targeted transformation of S100B cells generates animal gliomas (Weiss et al. 2003) and S100B promoter reporter models demonstrate some co-expression of S100B and NG2 in AGPs (Hachem et al. 2005), S100B cells do not appear to significantly contribute to the proliferative population of human glioma cells. In the present study, the lack of S100B, but abundant Olig2 expression in proliferating cells from the same samples, suggests that Olig2/Mib-1 defines a distinct mitotic cell type unrelated to the S100B cells described as oligodendroglial progenitors in animal studies (Weiss et al 2003; Hachen et al 2005). We

were unable to perform Olig2 and S100B co-expression analysis because our Olig2 and S100B antibodies are raised in the same host species, but we did demonstrate that another astroglial marker, GFAP, which colocalizes strongly with S100B, appears to be virtually absent from both proliferating cells and Olig2 cells in non-neoplastic brain and gliomas. Together these observations support the possibility that mitotic Olig2 AGPs are preferential targets for human gliomagenesis or that the Olig2 AGP cellular phenotype is preferentially recapitulated in mitotic human glial tumor cells.

The roles of Olig2 AGPs in glioma biology

I. Glioma Histogenesis—The findings of this study demonstrated the relevance of the Olig2 AGP as a potential target cell for human gliomagenesis. First, the estimated prevalence of 10 million mitotic Olig2 AGPs in adult human neocortical GM and SCWM demonstrated their numerical relevance. In addition, the presence of Olig2/Mib-1 cells in all differentiated glioma sub-types (astrocytic, oligodendroglial and mixed oligoastrocytic) recapitulates their normal multi-potent differentiation potential (Nunes et al. 2003) (Marshall et al. 2005). Finally, their capacity for proliferation fulfills an important precondition for malignant transformation by permitting propagation of oncogenic mutations and genomic instability, a hallmark feature of cancer cells (Beckman and Loeb 2005; Hanahan and Weinberg 2000; Loeb and Loeb 2000). Of interest, unlike SVZ NSCs that decline in number, proliferation and self-renewal capacity with age (Molofsky et al, 2006), AGP numbers may actually increase in the adult (Dawson et al, 2003). Given that the age-adjusted incidence of adult human gliomas steadily increases over time (CBTRUS 2005), and mirrors the acquisition of genetic instability with age in rodent neural progenitors (Bailey et al, 2004), future analysis of age-related changes in the prevalence of mitotic AGPs versus NSCs may provide important insight into their relative roles in gliomagensis.

Our data suggests that AGPs are a likely target for glioma histogenesis, but NSCs are also a potential cell of origin. Although CD133 has shown promise, the recent identification of CD133-negative tumor stem cells in glioblastomas underscores the lack of an unambiguous *in vivo* glioma stem cell marker (Beier et al, 2007). Not surprisingly, neural stem cell markers (CD133, Nestin, Musashi-1, Sox2) exhibit variable expression patterns in human glioma samples and importantly none co-localize with Mib-1 (Ma et al, 2008). Future studies to determine the identity of the Olig2−/Mib-1+ population will establish the relative prevalence of a stem cell versus AGP immunophenotype in human gliomas and provide additional insight into human glioma histogenesis.

II. Recruitment of Endogenous AGPs—An alternative interpretation of our results is based on the notion that gliomas can activate proliferation and recruitment of endogenous AGPs to the tumor. In a murine model of primary glioblastoma, Assanah et al, show that less than 20% of tumor cells were target cells infected by oncogenic retrovirus, and that the vast majority of the total and proliferating cell population had an Olig2 or A2B5 AGP immunophenotype (Assanah et al. 2006). Ikovic et al, also observed a similar phenomenon they termed “progenitor hyperplasia” in an EGFR driven animal model (Ikovic et al. 2008). Glass et al, further showed that the degree of endogenous neural progenitor cell recruitment to the tumor is inversely related to host age but directly related to improved survival (Glass

et al. 2005). These findings suggest that the decrease in Olig2/Mib-1 LI observed here and total Olig2 expression in grade IV versus grade II and III tumors documented by many others (Mokhtari et al 2005; Aguirre-Cruz et al 2005; Ohnishi et al 2003) could, in part, reflect decreased recruitment of endogenous Olig2 AGPs by GBMs. The potential clinical relevance of endogenous neural progenitor recruitment warrants further investigation that will require development of techniques to distinguish Olig2/Mib-1glioma cells from recruited AGPs.

III. Glioma Pathogenesis—An overall reduction in Olig2 expression, irrespective of its localization in mitotic cells, is noted in multiple studies of grade IV tumors compared to lower grade tumors (Mokhtari et al. 2005; Aguirre-Cruz et al. 2005; Ohnishi et al. 2003). The decreased expression of Olig2 in grade IV gliomas brings up the possibility that Olig2 may function to suppress features of a malignant phenotype. Our finding that the mean Olig2/Mib-1 LI decreased from 67.7% for grade II and 83.5% for grade III gliomas to 24% for grade IV GBMs also supported an inverse correlation between Olig2 expression and Olig2 AGP prevalence and malignant glioma phenotype. For instance, Tabu et al, show that Olig2 suppresses cell proliferation, migration and anchorage independent growth in malignant glioma cells by activation of Rho A and the cyclin-dependent kinase inhibitor p27 (Tabu et al. 2006, 2007). Of note, increased p27 expression in human glioma samples correlates with better patient outcome and lower tumor grade (Cavalla et al. 1999; Kirla et al. 2003; Mizumatsu et al. 1999; Tamiya et al. 2001; Zagzag et al. 2003). In addition microarray studies demonstrate that loss of Olig2 expression is characteristic of progression from a prognostically favorable “pro-neural” glioma sub-type to a more aggressive “mesenchymal” glioma phenotype (Phillips et al. 2006). Of interest, the “pro-neural” glioma sub-type is characterized by activation of the Notch signaling (Phillips et al. 2006) that is also a feature of Olig2/LMO1 driven leukemogenesis (Lin et al, 2005). Together these observations suggest that in gliomas Olig2 may participate in tumor formation but that its loss may permit or contribute to more malignant phenotypes.

In contrast, Ligon et al demonstrate a requirement of Olig2 for gliomagenesis from neural progenitor cells associated with suppression of p21 (but not activation of p27) that contributes to a more malignant phenotype (Ligon et al. 2007). This same study reports an Olig2/Ki67 LI of ~85% by FACS in 11 GBM samples confirmed by IHC as 85% from 3 GBM samples (Ligon et al. 2007). The differences in this report and the present study related to Olig2/Mib-1 LIs in GBM may reflect the highly heterogeneous nature of these neoplasms and their distinct molecular sub-types. Additional analysis of a larger series of glioma samples defined more rigorously by clinical, molecular and neuropathologic features is required to better define the clinical relevance of the mitotic Olig2 cell and its prevalence in human gliomas. The apparent conflicting functional roles reported for Olig2 in malignant glioma biology also require clarification. Future studies should account for the possibility that the functional impact of Olig2 is context-dependent, related to the stage of tumorigenesis or progression and the molecular/clinical glioma sub-type.

SUMMARY

This study quantified mitotic cells with Olig2 AGP phenotype in non-neoplastic human brain outside the germinative zones and a full spectrum of human gliomas. Olig2 marks the majority of mitotic cells in non-neoplastic brain, particularly in white matter and provides a numerically large pool of potential targets for gliomagenesis and/or endogeneous activation that can contribute to the overall physiology of human gliomas. Within human gliomas, Olig2 cells represented a high proportion of mitotic cells of grade II and III tumors but a lesser minority in grade IV GBM. Future studies are required to probe the significance of this disparity. Characterizing Olig2 function and the role of Olig2 AGPs in animal models of gliomagenesis will add to our understanding of glioma biology, generate relevant pre-clinical models of human gliomas and reveal novel targets for glioma therapy.

Supplementary Material

Refer to Web version on PubMed Central for supplementary material.

Acknowledgements

The authors thank Mei Deng for her technical assistance with the immunohistochemistry and Jason Barber and Nancy Temkin for their assistance with statistical analyses of the data. This study was funded by the NIH T32NS0007144 Clinical Neuroscience Training Grant and the University of Washington Royalty Research Fund Proposal #3611.

References

Aguirre-Cruz L, Mokhtari K, Hoang-Xuan K, Marie Y, Criniere E, Taillibert S, Lopes M, Delattre JY, Sanson M. Analysis of the bHLH transcription factors Olig1 and Olig2 in brain tumors. J Neurooncol. 2004; 67(3):265–271. [PubMed: 15164981]

Arsenijevic Y, Villemure JG, Brunet JF, Bloch JJ, Déglon N, Kostic C, Zurn A, Aebischer P. Isolation of multipotent neural precursors residing in the cortex of the adult human brain. Exp Neurol. 2001; 170(1):48–62. [PubMed: 11421583]

Assanah M, Lochhead R, Ogden A, Bruce J, Goldman J, Canoll P. Glial progenitors in adult white matter are driven to form malignant gliomas by platelet-derived growth factor-expressing retroviruses. J Neurosci. 2006; 26(25):6781–6790. 2006. [PubMed: 16793885]

Bailey KJ, Maslov AY, Pruitt SC. Accumulation of mutations and somatic selection in aging neural stem/progenitor cells. Aging Cell. 2004; 3(6):391–397. [PubMed: 15569356]

Barnett SC, Robertson L, Graham D, Allan D, Rampling R. Oligodendrocyte-type-2 astrocyte (O-2A) progenitor cells transformed with c-myc and H-ras form high-grade glioma after stereotactic injection into the rat brain. Carcinogenesis. 1998; 19(9):1529–1537. [PubMed: 9771921]

Beckman RA, Loeb LA. Genetic instability in cancer: theory and experiment. Semin Cancer Biol. 2005; 15(6):423–435. [PubMed: 16043359]

Beier D, Hau P, Proescholdt M, Lohmeier A, Wischhusen J, Oefner PJ, Aigner L, Brawanski A, Bogdahn U, Beier CP. CD133(+) and CD133(−) glioblastoma-derived cancer stem cells show differential growth characteristics and molecular profiles. Cancer Res. 2007; 67(9):4010–4015. [PubMed: 17483311]

Boyes BE, Kim SU, Lee V, Sung SC. Immunohistochemical co-localization of S-100b and the glial fibrillary acidic protein in rat brain. Neuroscience. 1986; 17(3):857–865. [PubMed: 2422599]

Camby I, Nagy N, Lopes MB, Schafer BW, Maurage CA, Ruchoux MM, Murmann P, Pochet R, Heizmann CW, Brotchi J, et al. Supratentorial pilocytic astrocytomas, astrocytomas, anaplastic astrocytomas and glioblastomas are characterized by a differential expression of S100 proteins. Brain Pathol. 1999; 9(1):1–19. [PubMed: 9989446]

Cavalla P, Piva R, Bortolotto S, Grosso R, Cancelli I, Chio A, Schiffer D. p27/kip1 expression in oligodendrogliomas and its possible prognostic role. Acta Neuropathol (Berl). 1999; 98(6):629–634. [PubMed: 10603039]

CBTRUS. Statistical Report: Primary brain tumors in the United States, 1998–2002. 2005.

Chang A, Nishiyama A, Peterson J, Prineas J, Trapp BD. NG2-positive oligodendrocyte progenitor cells in adult human brain and multiple sclerosis lesions. J Neurosci. 2000; 20(17):6404–6412. [PubMed: 10964946]

Colin C, Virard I, Baeza N, Tchoghandjian A, Fernandez C, Bouvier C, Calisti A, Tong S, Durbec P, Figarella-Branger D. Relevance of combinatorial profiles of intermediate filaments and transcription factors for glioma histogenesis. Neuropathol Appl Neurobiol. 2007; 33(4):431–439. [PubMed: 17442061]

Dam AM. Neuropathology of epilepsy. Acta Neurochir Suppl (Wien). 1990; 50:20–25. [PubMed: 2129089]

Dawson MR, Polito A, Levine JM, Reynolds R. NG2-expressing glial progenitor cells: an abundant and widespread population of cycling cells in the adult rat CNS. Mol Cell Neurosci. 2003; 24(2): 476–488. [PubMed: 14572468]

Deloulme JC, Raponi E, Gentil BJ, Bertacchi N, Marks A, Labourdette G, Baudier J. Nuclear expression of S100B in oligodendrocyte progenitor cells correlates with differentiation toward the oligodendroglial lineage and modulates oligodendrocytes maturation. Mol Cell Neurosci. 2004; 27(4):453–465. [PubMed: 15555923]

Gensert JM, Goldman JE. Heterogeneity of cycling glial progenitors in the adult mammalian cortex and white matter. J Neurobiol. 2001; 48(2):75–86. [PubMed: 11438938]

Glass R, Synowitz M, Kronenberg G, Walzlein JH, Markovic DS, Wang LP, Gast D, Kiwit J, Kempermann G, Kettenmann H. Glioblastoma-induced attraction of endogenous neural precursor cells is associated with improved survival. J Neurosci. 2005; 25(10):2637–2646. [PubMed: 15758174]

Goldman S. Glia as neural progenitor cells. Trends Neurosci. 2003; 26(11):590–596. [PubMed: 14585598]

Hachem S, Aguirre A, Vives V, Marks A, Gallo V, Legraverend C. Spatial and temporal expression of S100B in cells of oligodendrocyte lineage. Glia. 2005; 51(2):81–97. [PubMed: 15782413]

Hanahan D, Weinberg RA. The hallmarks of cancer. Cell. 2000; 100(1):57–70. [PubMed: 10647931]

Hayashi K, Hoshida Y, Horie Y, Takahashi K, Taguchi K, Sonobe H, Ohtsuki Y, Akagi T. Immunohistochemical study on the distribution of alpha and beta subunits of S-100 protein in brain tumors. Acta Neuropathol (Berl). 1991; 81(6):657–663. [PubMed: 1882640]

Holland EC. Progenitor cells and glioma formation. Curr Opin Neurol. 2001; 14(6):683–688. [PubMed: 11723374]

Horner PJ, Thallmair M, Gage FH. Defining the NG2-expressing cell of the adult CNS. J Neurocytol. 2002; 31(6–7):469–480. [PubMed: 14501217]

Ivkovic S, Canoll P, Goldman JE. Constitutive EGFR signaling in oligodendrocyte progenitors leads to diffuse hyperplasia in postnatal white matter. J Neurosci. 2008; 28(4):914–922. [PubMed: 18216199]

Kato S, Esumi H, Hirano A, Kato M, Asayama K, Ohama E. Immunohistochemical expression of inducible nitric oxide synthase (iNOS) in human brain tumors: relationships of iNOS to superoxide dismutase (SOD) proteins (SOD1 and SOD2), Ki-67 antigen (MIB-1) and p53 protein. Acta Neuropathol (Berl). 2003; 105(4):333–340. [PubMed: 12624786]

Kendal C, Everall I, Polkey C, Al-Sarraj S. Glial cell changes in the white matter in temporal lobe epilepsy. Epilepsy Res. 1999; 36(1):43–51. [PubMed: 10463849]

Kirla RM, Haapasalo HK, Kalimo H, Salminen EK. Low expression of p27 indicates a poor prognosis in patients with high-grade astrocytomas. Cancer. 2003; 97(3):644–648. [PubMed: 12548606]

Kretschmann HJ, Kammradt G, Krauthausen I, Sauer B, Wingert F. Brain growth in man. Bibl Anat. 1986; (28):1–26. [PubMed: 3707509]

Kros JM, Schouten WC, Janssen PJ, van der Kwast TH. Proliferation of gemistocytic cells and glial fibrillary acidic protein (GFAP)-positive oligodendroglial cells in gliomas: a MIB-1/GFAP double labeling study. Acta Neuropathol (Berl). 1996; 91(1):99–103. [PubMed: 8773153]

Krtolica A. Stem cell: balancing aging and cancer. Int J Biochem Cell Biol. 2005; 37(5):935–941. [PubMed: 15743668]

Ligon KL, Alberta JA, Kho AT, Weiss J, Kwaan MR, Nutt CL, Louis DN, Stiles CD, Rowitch DH. The oligodendroglial lineage marker OLIG2 is universally expressed in diffuse gliomas. J Neuropathol Exp Neurol. 2004; 63(5):499–509. [PubMed: 15198128]

Ligon KL, Fancy SP, Franklin RJ, Rowitch DH. Olig gene function in CNS development and disease. Glia. 2006a; 54(1):1–10. [PubMed: 16652341]

Ligon KL, Kesari S, Kitada M, Sun T, Arnett HA, Alberta JA, Anderson DJ, Stiles CD, Rowitch DH. Development of NG2 neural progenitor cells requires Olig gene function. Proc Natl Acad Sci U S A. 2006b; 103(20):7853–7858. [PubMed: 16682644]

Ligon KL, Huillard E, Mehta S, Kesari S, Liu H, Alberta JA, Bachoo RM, Kane M, Louis DN, Depinho RA, Anderson DJ, Stiles CD, Rowitch DH. Olig2-regulated lineage-restricted pathway controls replication competence in neural stem cells and malignant glioma. Neuron. 2007; 53(4): 503–517. [PubMed: 17296553]

Lin YW, Deveney R, Barbara M, Iscove NN, Nimer SD, Slape C, Aplan PD. OLIG2 (BHLHB1), a bHLH transcription factor, contributes to leukemogenesis in concert with LMO1. Cancer Res. 2005; 65(16):7151–7158. [PubMed: 16103065]

Liu Y, Rao MS. Glial progenitors in the CNS and possible lineage relationships among them. Biol Cell. 2004; 96(4):279–290. [PubMed: 15145532]

Loeb KR, Loeb LA. Significance of multiple mutations in cancer. Carcinogenesis. 2000; 21(3):379–385. [PubMed: 10688858]

Ma YH, Mentlein R, Knerlich F, Kruse ML, Mehdorn HM, Held-Feindt J. Expression of stem cell markers in human astrocytomas of different WHO grades. J Neurooncol. 2008; 86(1):31–45. [PubMed: 17611714]

Marshall CA, Novitch BG, Goldman JE. Olig2 directs astrocyte and oligodendrocyte formation in postnatal subventricular zone cells. J Neurosci. 2005; 25(32):7289–7298. [PubMed: 16093378]

Menn B, Garcia-Verdugo JM, Yaschine C, Gonzalez-Perez O, Rowitch D, Alvarez-Buylla A. Origin of oligodendrocytes in the subventricular zone of the adult brain. J Neurosci. 2006; 26(30):7907–7918. [PubMed: 16870736]

Mesiwala AH, Scampavia LD, Rabinovitch PS, Ruzicka J, Rostomily RC. On-line flow cytometry for real-time surgical guidance. Neurosurgery. 2004; 55(3):551–560. discussion 560-1. [PubMed: 15335422]

Miller AK, Alston RL, Corsellis JA. Variation with age in the volumes of grey and white matter in the cerebral hemispheres of man: measurements with an image analyser. Neuropathol Appl Neurobiol. 1980; 6(2):119–132. [PubMed: 7374914]

Mizumatsu S, Tamiya T, Ono Y, Abe T, Matsumoto K, Furuta T, Ohmoto T. Expression of cell cycle regulator p27Kip1 is correlated with survival of patients with astrocytoma. Clin Cancer Res. 1999; 5(3):551–557. [PubMed: 10100706]

Mokhtari K, Paris S, Aguirre-Cruz L, Privat N, Criniere E, Marie Y, Hauw JJ, Kujas M, Rowitch D, Hoang-Xuan K, et al. Olig2 expression, GFAP, p53 and 1p loss analysis contribute to glioma subclassification. Neuropathol Appl Neurobiol. 2005; 31(1):62–69. [PubMed: 15634232]

Molofsky AV, Slutsky SG, Joseph NM, He S, Pardal R, Krishnamurthy J, Sharpless NE, Morrison SJ. Increasing p16INK4a expression decreases forebrain progenitors and neurogenesis during ageing. Nature. 2006; 443(7110):448–452. [PubMed: 16957738]

Mouritzen Dam A. Shrinkage of the brain during histological procedures with fixation in formaldehyde solutions of different concentrations. J Hirnforsch. 1979; 20(2):115–119. [PubMed: 556570]

Nedergaard M, Astrup J, Klinken L. Cell density and cortex thickness in the border zone surrounding old infarcts in the human brain. Stroke. 1984; 15(6):1033–1039. [PubMed: 6209831]

Nunes MC, Roy NS, Keyoung HM, Goodman RR, McKhann G 2nd, Jiang L, Kang J, Nedergaard M, Goldman SA. Identification and isolation of multipotential neural progenitor cells from the subcortical white matter of the adult human brain. Nat Med. 2003; 9(4):439–447. [PubMed: 12627226]

Ohnishi A, Sawa H, Tsuda M, Sawamura Y, Itoh T, Iwasaki Y, Nagashima K. Expression of the oligodendroglial lineage-associated markers Olig1 and Olig2 in different types of human gliomas. J Neuropathol Exp Neurol. 2003; 62(10):1052–1059. [PubMed: 14575240]

Pakkenberg B, Gundersen HJ. Neocortical neuron number in humans: effect of sex and age. J Comp Neurol. 1997; 384(2):312–320. [PubMed: 9215725]

Park SH, Suh YL. Expression of cyclin A and topoisomerase IIalpha of oligodendrogliomas is correlated with tumour grade, MIB-1 labelling index and survival. Histopathology. 2003; 42(4): 395–402. [PubMed: 12653952]

Pelvig DP, Pakkenberg H, Regeur L, Oster S, Pakkenberg B. Neocortical glial cell numbers in Alzheimer's disease. A stereological study. Dement Geriatr Cogn Disord. 2003; 16(4):212–219. [PubMed: 14512716]

Phillips HS, Kharbanda S, Chen R, Forrest WF, Soriano RH, Wu TD, Misra A, Nigro JM, Colman H, Soroceanu L, et al. Molecular subclasses of high-grade glioma predict prognosis, delineate a pattern of disease progression, and resemble stages in neurogenesis. Cancer Cell. 2006; 9(3):157–173. [PubMed: 16530701]

Rostomily RC, Hoyt JW, Berger MS, Kros JM, Alvord EC, Wilkins P, Rabinovitch P. Pleomorphic xanthoastrocytoma: DNA flow cytometry and outcome analysis of 12 patients. Cancer. 1997; 80(11):2141–2150. [PubMed: 9392337]

Rousseau A, Nutt CL, Betensky RA, Iafrate AJ, Han M, Ligon KL, Rowitch DH, Louis DN. Expression of oligodendroglial and astrocytic lineage markers in diffuse gliomas: use of YKL-40, ApoE, ASCL1, and NKX2-2. J Neuropathol Exp Neurol. 2006; 65(12):1149–1156. [PubMed: 17146289]

Schnell SA, Staines WA, Wessendorf MW. Reduction of lipofuscin-like autofluorescence in fluorescently labeled tissue. J Histochem Cytochem. 1999; 47(6):719–730. [PubMed: 10330448]

Scolding NJ, Rayner PJ, Compston DA. Identification of A2B5-positive putative oligodendrocyte progenitor cells and A2B5-positive astrocytes in adult human white matter. Neuroscience. 1999; 89(1):1–4. [PubMed: 10051212]

Scolding NJ, Rayner PJ, Sussman J, Shaw C, Compston DA. A proliferative adult human oligodendrocyte progenitor. Neuroreport. 1995; 6(3):441–445. [PubMed: 7766839]

Sharpless NE, DePinho RA. Telomeres, stem cells, senescence, and cancer. J Clin Invest. 2004; 113(2):160–168. [PubMed: 14722605]

Shoshan Y, Nishiyama A, Chang A, Mork S, Barnett GH, Cowell JK, Trapp BD, Staugaitis SM. Expression of oligodendrocyte progenitor cell antigens by gliomas: implications for the histogenesis of brain tumors. Proc Natl Acad Sci U S A. 1999; 96(18):10361–10366. [PubMed: 10468613]

Tabu K, Ohnishi A, Sunden Y, Suzuki T, Tsuda M, Tanaka S, Sakai T, Nagashima K, Sawa H. A novel function of OLIG2 to suppress human glial tumor cell growth via p27Kip1 transactivation. J Cell Sci. 2006; 119(Pt 7):1433–1441. [PubMed: 16554441]

Tabu K, Ohba Y, Suzuki T, Makino Y, Kimura T, Ohnishi A, Sakai M, Watanabe T, Tanaka S, Sawa H. Oligodendrocyte lineage transcription factor 2 inhibits the motility of a human glial tumor cell line by activating RhoA. Mol Cancer Res. 2007; 5(10):1099–1109. [PubMed: 17951409]

Tamiya T, Mizumatsu S, Ono Y, Abe T, Matsumoto K, Furuta T, Ohmoto T. High cyclin E/low p27Kip1 expression is associated with poor prognosis in astrocytomas. Acta Neuropathol (Berl). 2001; 101(4):334–340. [PubMed: 11355304]

Van Eldik LJ, Jensen RA, Ehrenfried BA, Whetsell WO III. Immunohistochemical localization of S100 beta in human nervous system tumors by using monoclonal antibodies with specificity for the S100 beta polypeptide. J Histochem Cytochem. 1986; 34(8):977–982. [PubMed: 3734419]

Vives V, Alonso G, Solal AC, Joubert D, Legraverend C. Visualization of S100B–positive neurons and glia in the central nervous system of EGFP transgenic mice. J Comp Neurol. 2003; 457(4): 404–419. [PubMed: 12561079]

Weiss WA, Burns MJ, Hackett C, Aldape K, Hill JR, Kuriyama H, Kuriyama N, Milshteyn N, Roberts T, Wendland MF, et al. Genetic determinants of malignancy in a mouse model for oligodendroglioma. Cancer Res. 2003; 63(7):1589–1595. [PubMed: 12670909]

Wolf HK, Wiestler OD. Surgical pathology of chronic epileptic seizure disorders. Brain Pathol. 1993; 3(4):371–380. [PubMed: 8293193]

Yokoo H, Nobusawa S, Takebayashi H, Ikenaka K, Isoda K, Kamiya M, Sasaki A, Hirato J, Nakazato Y. Anti-human Olig2 antibody as a useful immunohistochemical marker of normal oligodendrocytes and gliomas. Am J Pathol. 2004; 164(5):1717–1725. [PubMed: 15111318]

Zagzag D, Blanco C, Friedlander DR, Miller DC, Newcomb EW. Expression of p27KIP1 in human gliomas: relationship between tumor grade, proliferation index, and patient survival. Hum Pathol. 2003; 34(1):48–53. [PubMed: 12605366]

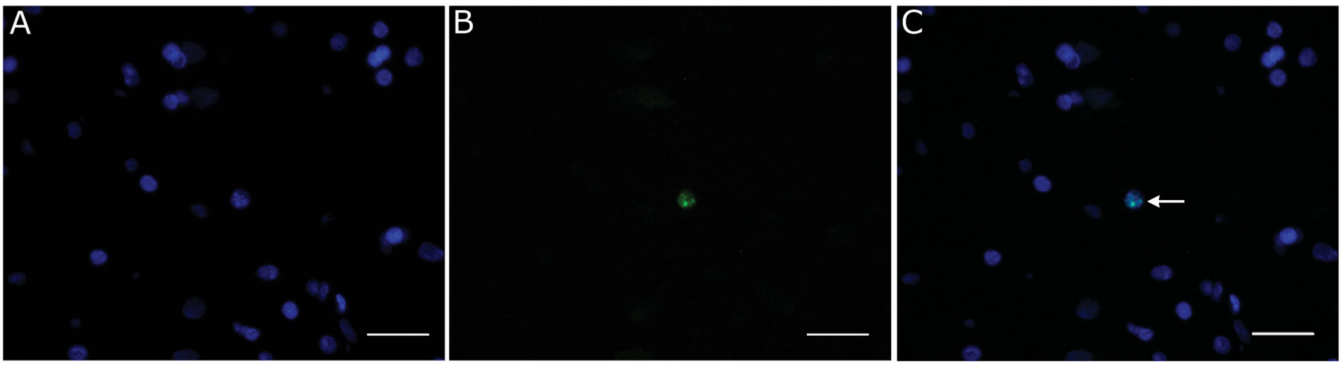

Figure 1.

Detection of mitotic cells in non-neoplastic human brain. Photomicrographs of a representative section of non-neoplastic human brain stained with DAPI (A), Mib-1 (B) and merged (C) showing nuclear localization of Mib-1 immunoreactivity (arrow). Scale bar= 3μm.

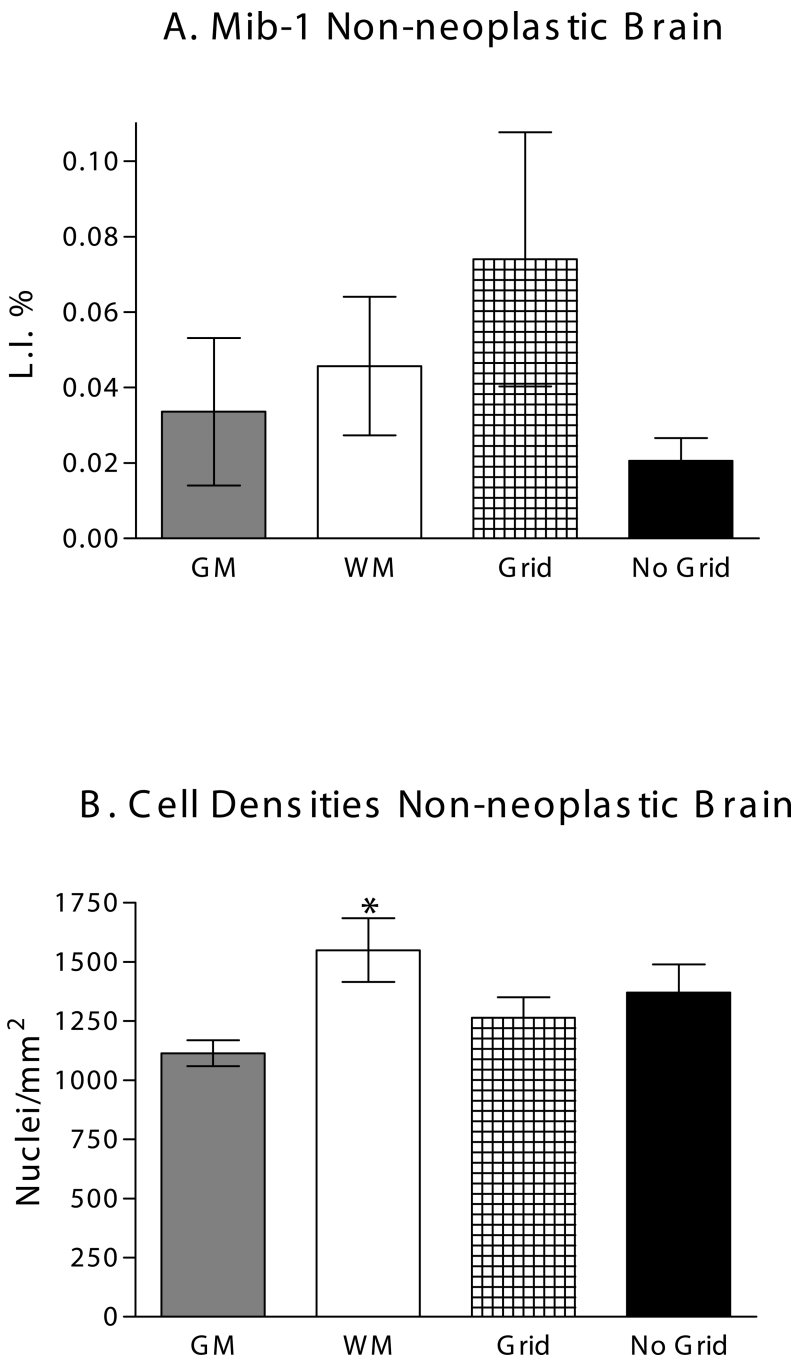

Figure 2.

Prevalence of mitotic Mib-1 immunoreactive cells and cell densities in non-neoplastic human brain. (A) The Mib-1 labeling index in samples of gray matter (GM) and white matter (WM; also referred to as SCWM) and in patients with (Grid) and without (No Grid) prior grid application. (B) Total cell densities from samples corresponding to those above (A) demonstrate increased cell density in WM versus GM that was statistically significant ($p<0.05$).

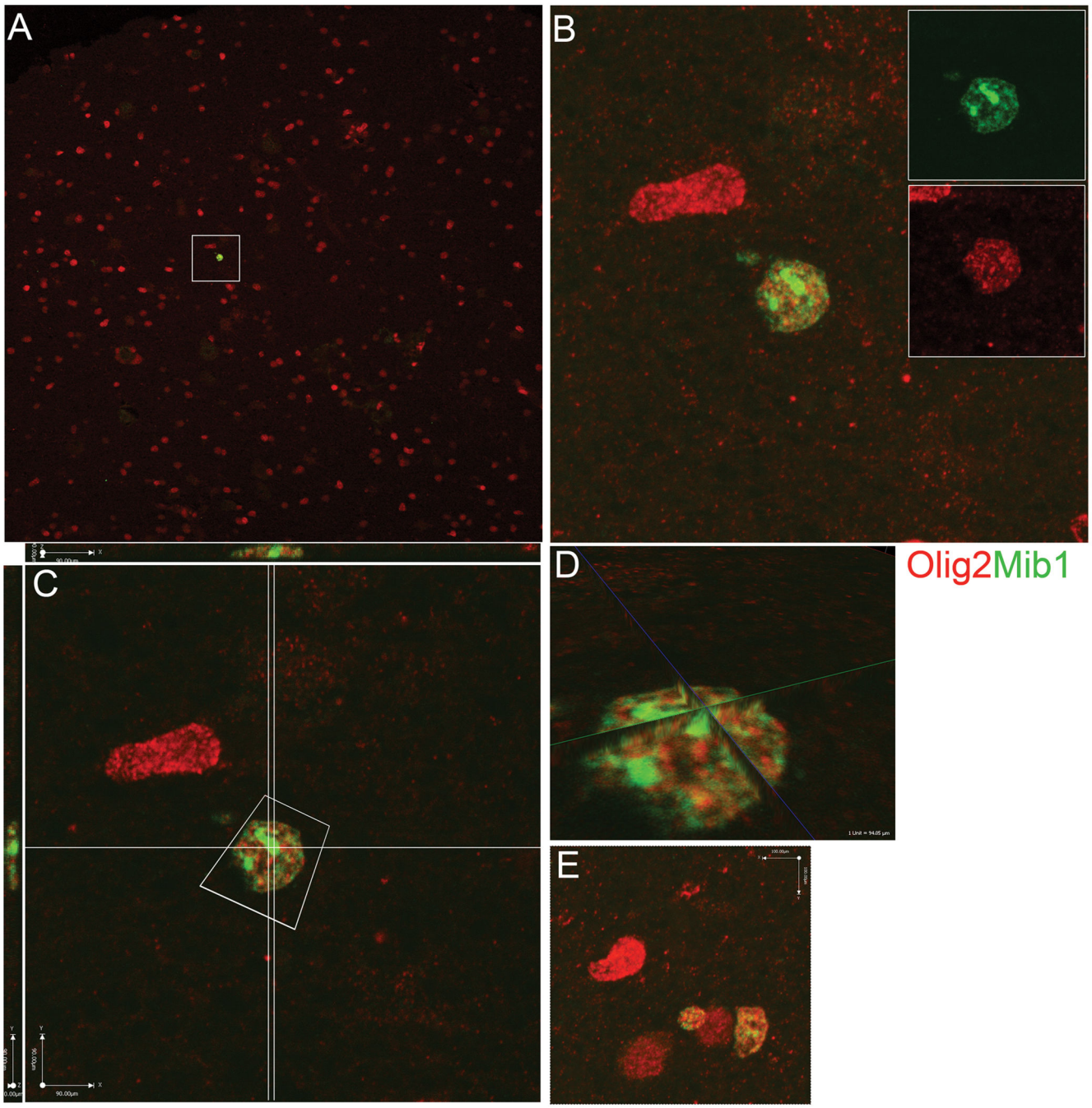

Figure 3.

Montage demonstrating Olig2 expression in mitotically active cells of non-neoplastic human brain. A) A 20× confocal image of non-neoplastic human brain labeled with Mib-1 (FITC) and Olig2 (rhodamine) demonstrates a double-labeled cell (outlined by box). B) 60 × confocal image of same area as in (A) showing two Olig2 cells, one of which co-expresses Mib-1. The inset shows the distinct specific immunofluorescent signals for Mib-1 (upper) and Olig2 (lower). C) Z-stack series of the same field demonstrates distinct non-overlapping signal for each antibody. D) A magnified view of the double-labeled cell shown in (C). E)

Image of single and double-labeled cells from a separate specimen. Scale bars: A) 80 μm; B) 8 μm; C) 10 μm E) 9 μm.

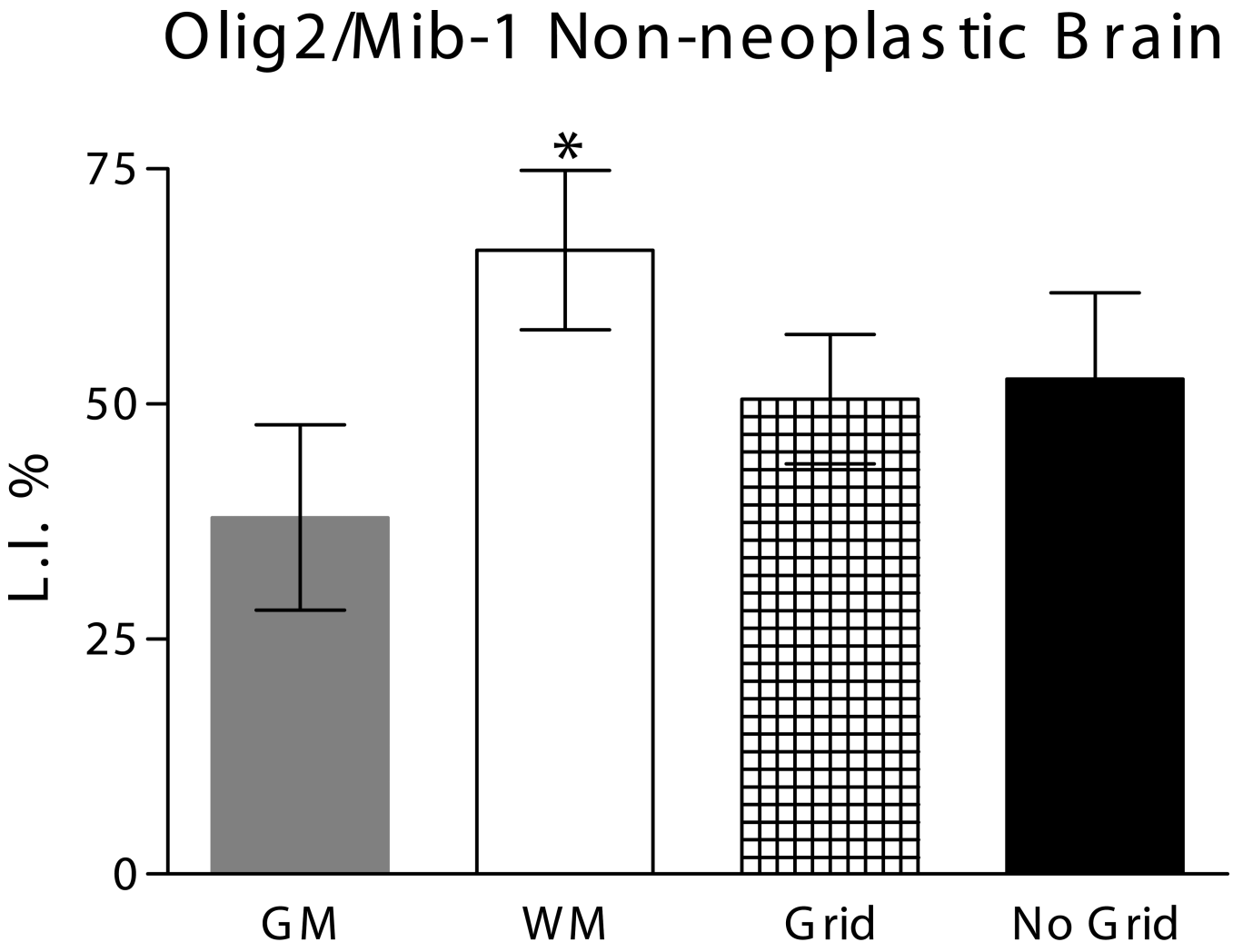

Figure 4.

Co-expression of Olig2 in Mib-1 immunoreactive cells. Histogram of the Olig2/Mib-1 labeling index expressed as a percentage for sub-groups of gray matter (GM), white matter (WM), prior and no grid samples. The LI was lower in GM than WM and this difference was statistically significant ($p<0.05$).

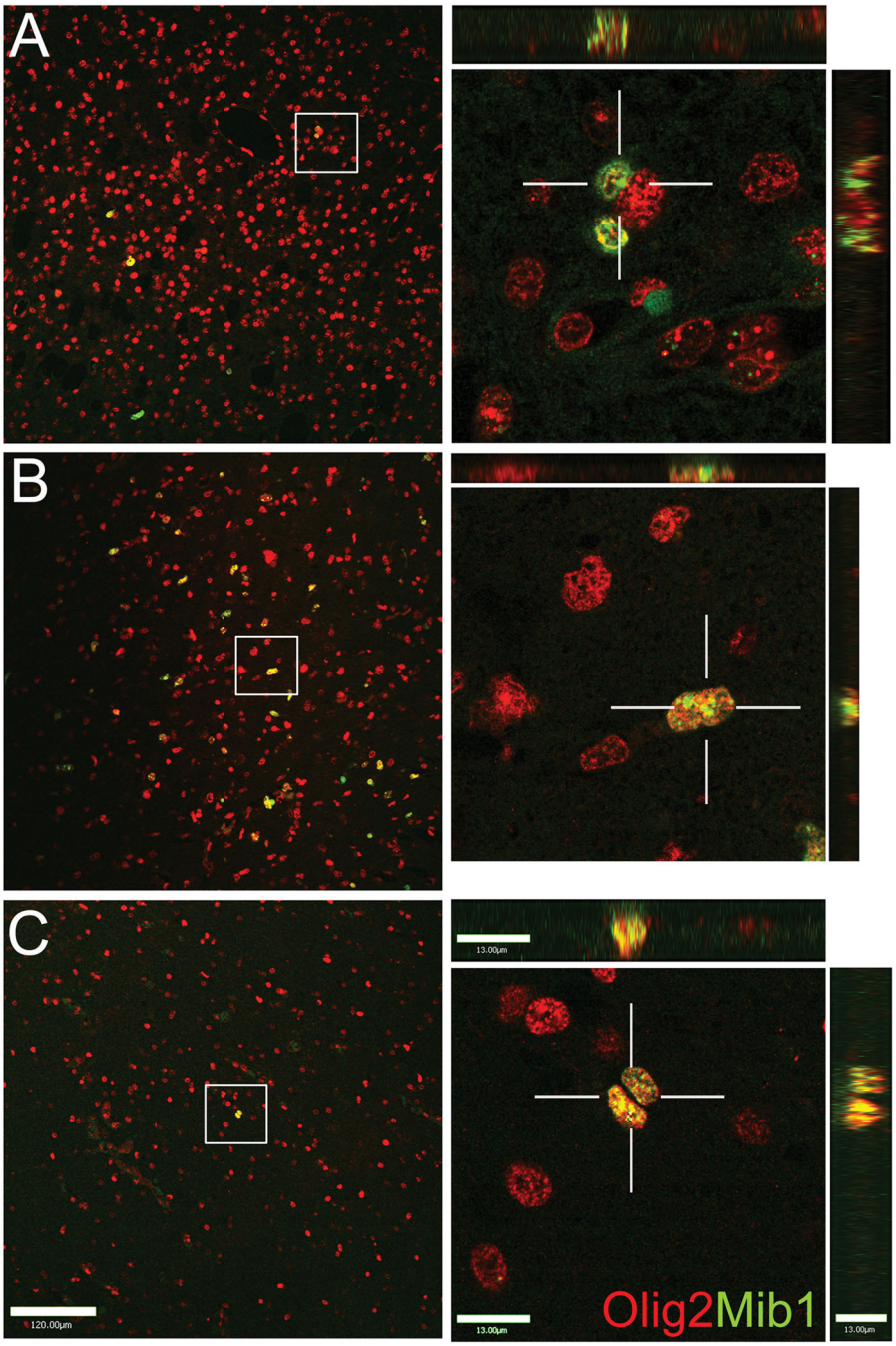

Figure 5.

Mitotic Olig2 cells in human gliomas. Representative confocal images of human glioma tumor samples double-labeled with Mib-1 (FITC) and Olig2 (rhodamine) are shown from a grade II oligodendroglioma (A), grade II astrocytoma (B) and grade IV GBM (C). Lower power 20× images (scale bar= 120 µm) are shown in the left panel and 60 × images (scale bar= 13 µm) are shown to the right.

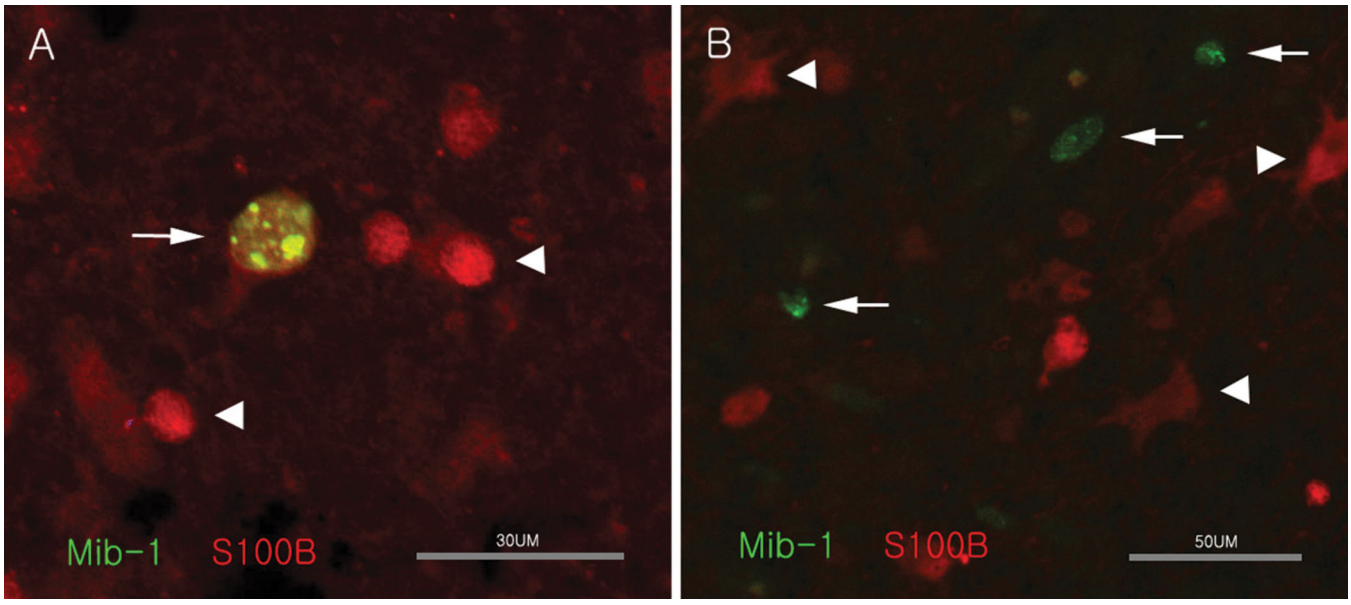

Figure 6.

S100B expression in mitotic human glioma cells. Representative 40× photomicrographs of grade II oligodendroglioma (A) and grade II astrocytoma (B) immunostained with S100B (rhodamine) and Mib-1 (FITC). A rare double-labeled cell is identified in (A) while Mib-1 immunoreactive cells (arrows) in (B) do not co-express S100B.

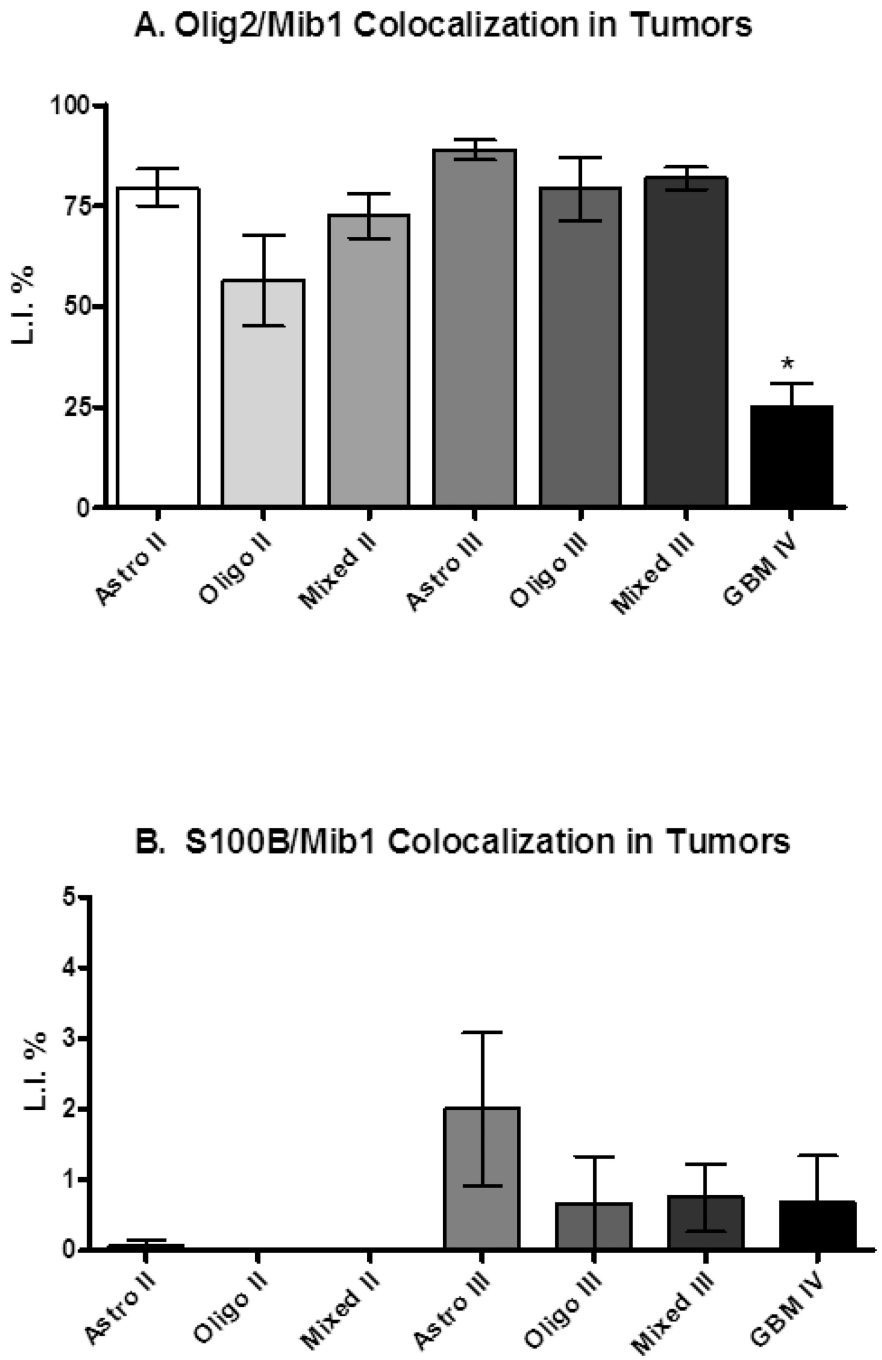

Figure 7.

Comparison of mitotic Olig2 and S100B cells in human gliomas of different type and grade. Histograms summarize labeling indices of double-labeled cells expressed as a percentage of total Mib-1 mitotic cells from grade II oligodendrogliomas (oligo II, n=5), grade II astrocytoma (astro II, n=4), grade II mixed oligoastrocytoma (mixed II, n=2), grade III oligodendrogliomas (oligo III, n=4), grade III astrocytoma (astro III, n=3), grade III mixed oligoastrocytoma (mixed III, n=4) and grade IV glioblastoma (GBM IV, n=9). Considered individually by sub-type, all grade II and grade III gliomas had significantly higher Olig2/

Mib-1 LI than grade IV GBM (Astro II $p<0.001$; Oligo II $p<0.05$; Mixed II $p<0.01$; Astro III $p<0.001$; Oligo III $p<0.001$; Mixed III $p<0.001$). S100B/Mib-1 cells were rarely identified and no statistically significant difference in S100B/Mib-1LI was detected between glioma sub-types or grades.

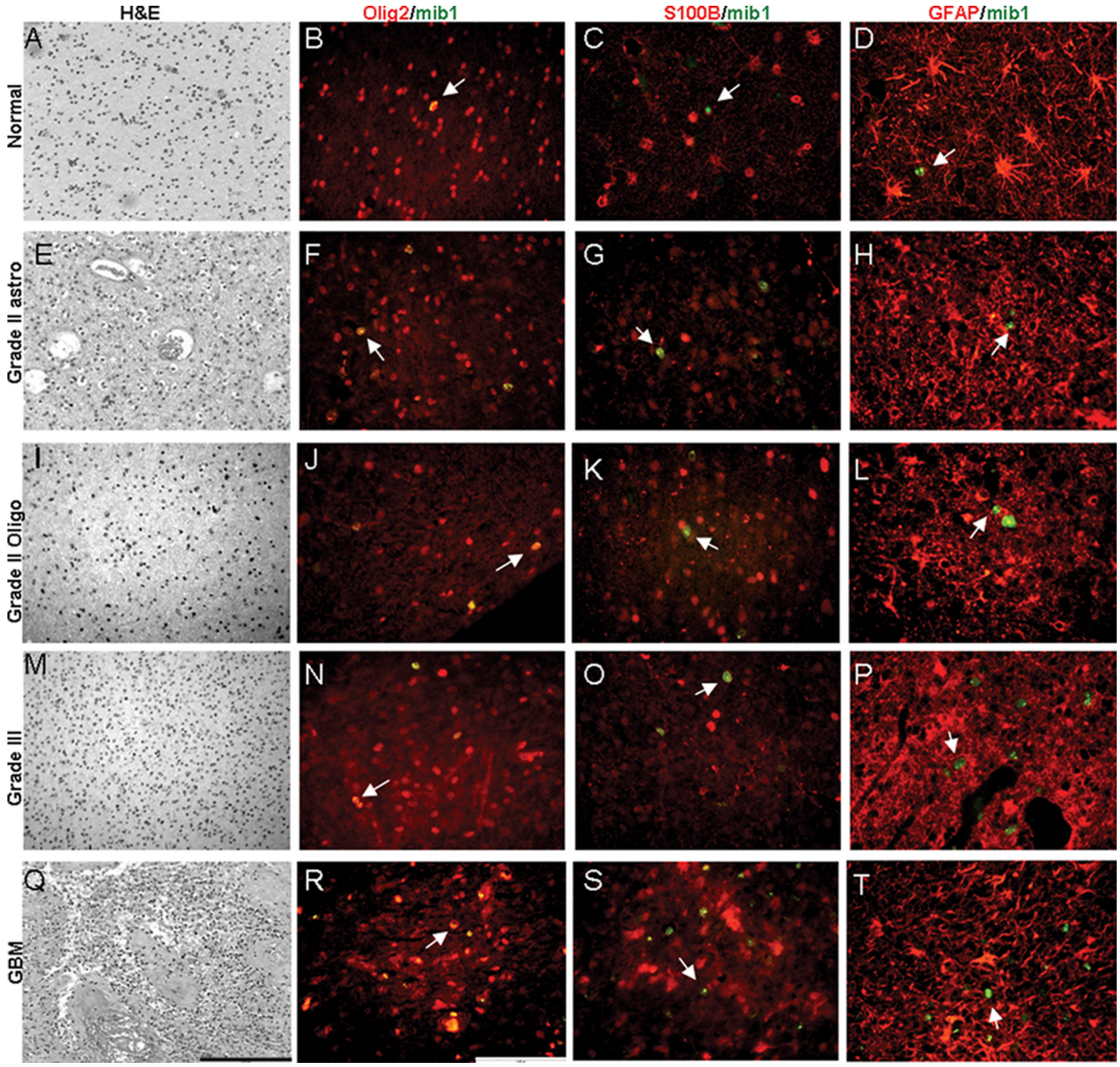

Figure 8.

Immunoprofile of proliferating cells in non-neoplastic brain and gliomas. Photomicrographs of adjacent sections from samples of non-neoplastic brain (A–D) and tumors (E–T) from human patients. All H&E sections are 20×, all IHC images are 40×, scale bars are shown in Q (10μm) and R (5μm). Olig2, S100 and GFAP are labeled with rhodamine (red) and Mib-1 is labled with FITC (green). One example of a Mib1 cell is shown by an arrow in each panel. Colabeled cells are yellow. Most proliferating cells in both non-neoplactic and neoplastic brain express Olig2 but not S100B or GFAP.

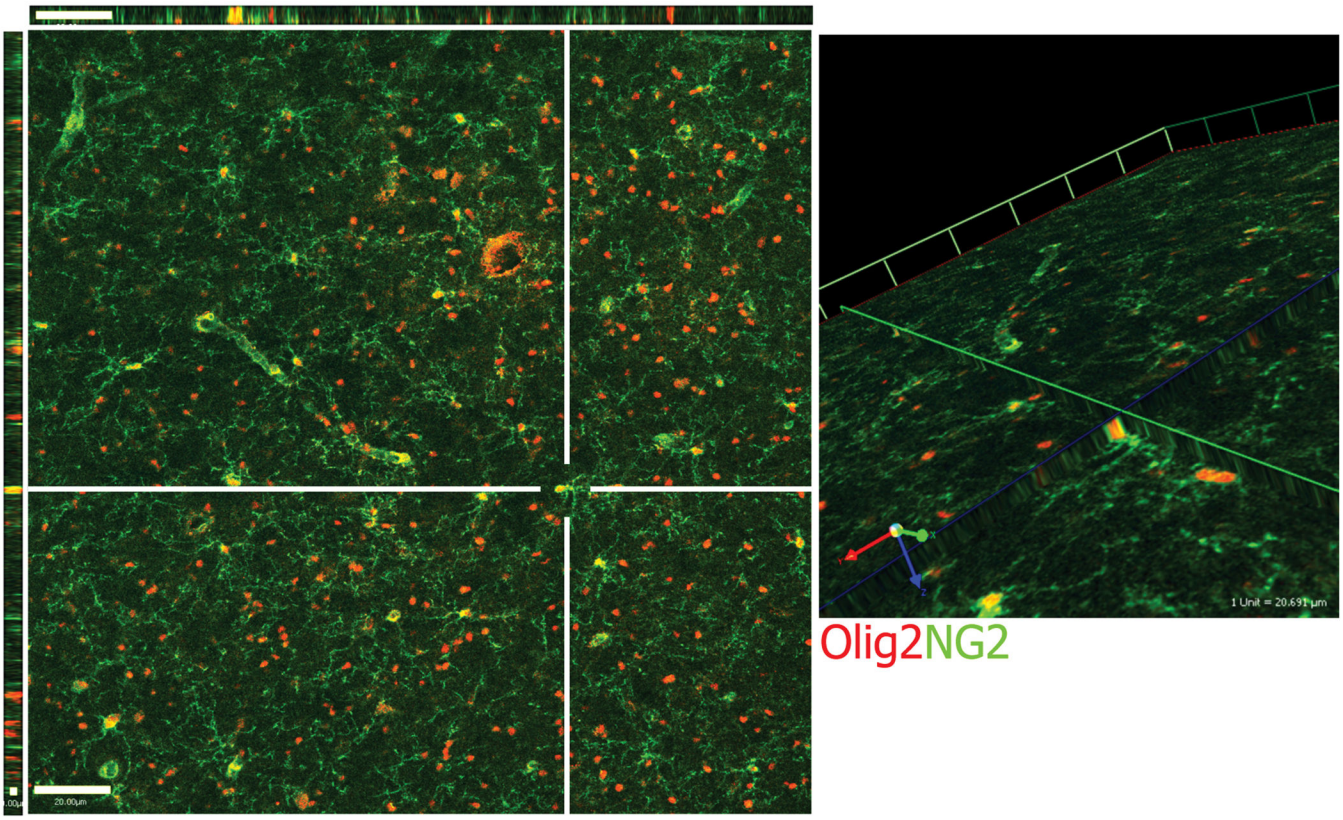

Figure 9.

Co-expression of Olig2 and NG2 in non-neoplastic human brain. Representative confocal microscopic image demonstrating co-expression of Olig2 (rhodamine) and NG2 (FITC) in section of non-neoplastic human brain. NG2 immunoreactivity is abundant in cell processes and also co-localizes with adjacent Olig2 immunoreactive nuclei. We detected Olig2 co-localization in 62% of cells where NG2 staining could be resolved to a particular cell body and nucleus. Scale bar = 20 μm.

Table 1

Patient Characteristics
Temporal Lobe Brain Samples

Panel 1 (Mib-1)

Sample #	Surgical Indication	Sex	Age	Side	Prior Grid
1	Epilepsy	F	40	L	YES
2	Tuberous sclerosis	M	18	L	YES
3	Epilepsy	M	35	L	YES
4	Epilepsy	F	40	L	YES
5	Epilepsy	F	44	R	YES
6	Epilepsy	M	50	R	NO
7	Epilepsy	M	46	L	NO
8	Epilepsy	F	46	L	NO
9	Epilepsy	F	38	L	NO
10	Hemangiopericytoma	M	47	L	NO
11	Epilepsy	F	49	L	NO
12	Meningioma	M	48	R	NO
13	Epilepsy	M	36	R	NO
14	Epilepsy	M	44	L	NO

Panel 2 (Olig2/Mib-1)

Sample #	Surgical Indication	Sex	Age	Side	Prior Grid
1	Meningioma	M	23	R	NO
2	Epilepsy	F	36	L	NO
3	Epilepsy	F	42	L	NO
4	Epilepsy	F	31	L	NO
5	Epilepsy	F	41	L	NO
6	Epilepsy	M	22	L	YES
7	Epilepsy	F	61	L	NO
8	Epilepsy	M	42	L	YES
9	Epilepsy	M	25	R	YES
10	Epilepsy	M	40	L	NO

Panel 2 (Olig2/Mib-1)

Sample #	Surgical Indication	Sex	Age	Side	Prior Grid
11	Epilepsy	F	35	L	NO
12	Epilepsy	F	30	L	NO

Table 2

Mib-1 Labeling Index in Non-neoplastic Brain

	Number	Mean Cell Density cells/mm2	Total # Cells	# Mib-1 cells	Samples with no Mib-1 cells	Mib-1 LI ^ Mean of individual samples
All Samples	28	1332	266087	149	9	0.040
Gray Matter	14	1114	104880	53	5	0.034
White Matter	14	1550*	161207	96	4	0.046
Grid						
Total	10	1264	88868	108	4	0.074
Gray Matter	5	1110	35180	46	2	0.072
White Matter	5	1417	53688	62	2	0.076
No-Grid						
Total	18	1367	177219	41	5	0.021
Gray Matter	9	1116	69700	7	3	0.012
White Matter	9	1624*	107519	34	2	0.029

Ll= labeling index

^ no significant differences between sub-groups for Mib-1 LI in non-neoplastic brain samples

* significant difference compared with all GM samples $p<0.05$

Glia. Author manuscript; available in PMC 2015 April 30.

Table 3

Immunophenotype of Mib-1 Cells in Non-neoplastic Human Brain and Gliomas

SAMPLE	N	Grade	OLIG2 Mib-1 Cells Total #	Olig2/Mib-1 Cells Total #	Mean Olig2/Mib-1 LI (%) Individual Samples	Olig2/Mib-1 Ll(%) Individual Values	S100B Mib-1 Cells Total #	S100B/Mib-1 Cells Total #	Mean S100B/Mib-1 LI (%) Individual Samples
Brain-All	24		255	136	52.2 ^				
Brain-GM	12		153	61	38				
Brain-WM	12		102	75	66.4				
Brain- Grid	6		81	42	55.2				
Brain- No grid	18		174	94	52.7				
Astrocytoma	4	II	989	801	79.5**	(68, 78, 82, 90)	1239	1	0.075
Oligodendroglioma	5	II	798	359	56.4*	(21, 49, 51, 76, 85)	1050	1	0.01
Mixed Oligoastrocytoma	2	II	322	233	72.5*	(67, 78)	300	0	0
All Grade II	11	II	2109	1393	67.7**		2589	2	0.03
Astrocytoma	4	III	339	355	88.8**	(83, 87, 95, 90)	249	8	2
Oligodendroglioma	3	III	300	238	79.3**	(81, 92, 65)	300	2	0.667
Mixed Oligoastrocytoma	4	III	400	327	81.8**	(78, 79, 80, 90)	400	3	0.75
All Grade III	11	III	1039	920	83.6**		949	13	1.182
GBM	9	IV	1604	429	24.5	(6, 11, 12, 14, 18, 27, 35, 38, 63)	2749	20	0.68

N=number

Ll= labeling index

GM= gray matter

WM= white matter

GBM= glioblastoma

^ no significant differences in Olig2/Mib-1 LI between sub-groups in non-neo plastic brain samples

* significant diference from GBM $p < 0.05$

** significant diference from GBM $p < 0.001$